An Atlantic influence on evaporation in the Orinoco and Amazon basins

Nicolás Duque-Gardeazabal[1,2], Andrew R. Friedman[1,2], and Stefan Brönnimann[1,2]

[1]Oeschger Centre for Climate Change Research, University of Bern, Bern, Switzerland.
[2]Institute of Geography, University of Bern, Bern, Switzerland.

Correspondence: Nicolás Duque-Gardeazabal (nicolas.duque@unibe.ch)

Abstract.

Tropical South America's hydroclimate is influenced by ocean-atmospheric oscillations. The physical mechanisms that tele-connect the Atlantic modes of variability with the soil moisture and evaporation of the region remain unclear. This study uses composites of reanalysis and satellite data to identify the processes linking land-surface anomalies and ocean modes. It shows that the Atlantic Meridional Mode (AMM) generates cross-equatorial wind anomalies that affect moisture convergence, in turn modifying the cloud cover, precipitation, radiation availability and hence evaporation. The anomalies have important geographical differences depending on the analysed season; they migrate from the east in Austral autumn towards central Amazon and western Orinoco in Austral spring. The Atlantic El Niño (Atl3) affects the Guianas and eastern Orinoco by means of pressure and trade wind variability. Evaporation is water- or energy-driven depending on the position of the Intertropical Convergence Zone (ITCZ), but the anomalies are controlled by the phase of each mode which alter water and radiation availability. Both Atlantic modes mainly impact regions different from those impacted by El Niño Southern Oscillation (ENSO), although northeast Brazil and the Guianas might experience overlapping effects. Therefore, these ocean-atmospheric modes impact the water and energy cycles and might influence regional climate extremes (e.g. droughts and floods), and are critical for achiving sustainable development (SDG).
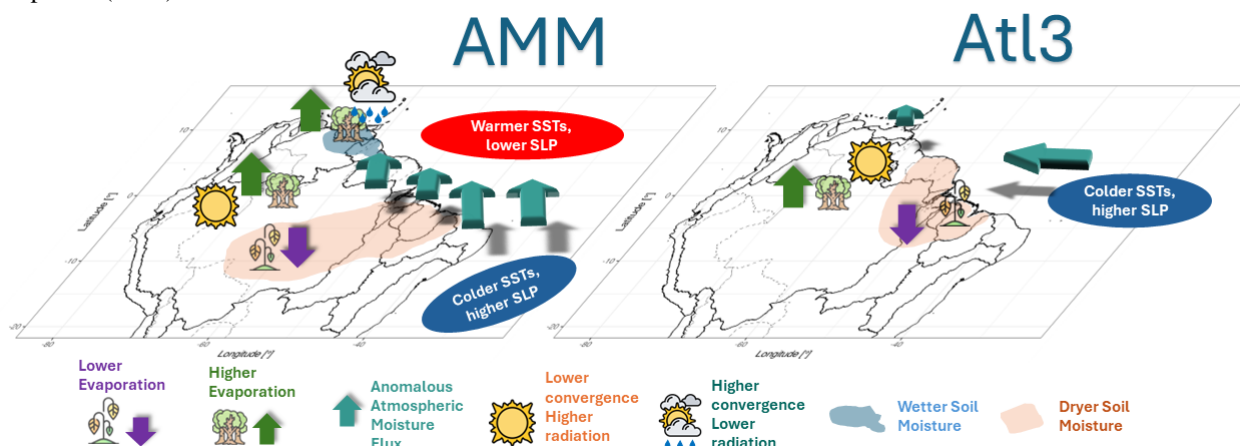
1 Introduction

The hydroclimate of Tropical South America is strongly influenced by ocean-atmospheric variability modes, for instance, El Niño/Southern Oscillation (ENSO) (Cai et al., 2020; Garreaud et al., 2009; Grimm and Zilli, 2009). Other variability sources stem from other ocean basins, Maidden-Julian Oscillations or local features like topography or land-atmosphere interactions (Pabón and Dorado, 2008; Cai et al., 2019). The modes cause their impact through atmospheric circulation anomalies; those anomalies enforce hydrological variability, which is evidenced by anomalies of precipitation, soil moisture (SM), temperature, evapotranspiration and streamflow. Among them, terrestrial evaporation is key for water, energy and carbon cycles (Wang and Dickinson, 2012). To predict ecosystem activity, it is essential to identify the evapotranspiration response to internal climate variability drivers (IPCC, 2021). The atmospheric anomalies might also influence extreme events (e.g. droughts and floods)(Merz et al., 2021; Mishra and Singh, 2010), and planning considering them is critical for achiving sustainable development.

Not only ENSO but also Atlantic Ocean modes are drivers of the regional atmospheric circulation (Lübbecke et al., 2018). Some studies statistically looked at the Pacific and Atlantic joint effects on precipitation (Gu and Adler, 2009; Ronchail et al., 2002), but the physical mechanism is still under research. Atlantic trade winds strength and the precipitation anomalies over South America are related to ocean variability modes such as: the Tropical North Atlantic mode (TNA)(Arias et al., 2015, 2020; Enfield, 1996), the Atlantic Meridional Mode (AMM) (Chiang et al., 2002; Fernandes et al., 2015; Rodrigues and McPhaden, 2014; Paccini et al., 2021; Drumond et al., 2014) and the Atlantic El Niño Equatorial mode (Atl3) (Ruiz-Barradas et al., 2000; Torralba et al., 2015; Vallès-Casanova et al., 2020). The Atlantic modes tend to be active and peak between the austral autumn and spring – MAM, JJA and SON, by the initial letters of the months – contrary to ENSO which peaks at the end of the year (SON and D(0)JF(+1)). These Atlantic modes might have contributed to northeast Brazil droughts and the Magdalena River floods in 2011-2012, besides the Amazon droughts in 2005 and 2010 (Lopes et al., 2016; Marengo and Espinoza, 2016). Although the Atlantic modes are associated with ENSO through atmospheric bridges or extratropical pathways (Compo and Sardeshmukh, 2010; Martín-Rey et al., 2014; García-Serrano et al., 2017), each of them has specific regional impacts on sea-level pressure (SLP) and hence on atmospheric circulation.

However, the physical mechanisms that teleconnect the Atlantic modes with the hydrological variability – especially with evapotranspiration – remain unclear. Some studies have statistically investigated ENSO's (Moura et al., 2019; Le and Bae, 2020; Miralles et al., 2014) or Atlantic modes' teleconnections with the evaporation in South America (Martens et al., 2018), but the physical reasons for these connections are not known. Some research has addressed the interannual changes in moisture transport, convergence, cloudiness and associated rainfall in the region (Hoyos et al., 2019; Cai et al., 2020; Ruiz-Vásquez et al., 2024). Arias et al. (2020) performed moisture transport analysis for the Amazon arc of deforestation and Orinoco and found correlations between the TNA, NDVI and precipitation over the Amazon. Atmospheric circulation variability produced

by the Atlantic SST modes is poorly understood, especially over the north (Orinoco basin). Evapotranspiration has received less attention.

Therefore, this study aims to investigate the physical reasons that cause the link between the AMM and Atl3 with the evaporation in tropical South America, at seasonal scale. Previous research has established SM and Net Radiation as the primary evaporation drivers in the atmosphere and the land-surface (Seneviratne et al., 2010; Hirschi et al., 2014); consequently, evaporation is classified into two regimes: water- or energy-limited. We specifically focus on:

1. determining where and when evaporation is dominated by a water- or energy-limited regime

2. establishing the chain of events that link the Atlantic modes to anomalies in atmospheric and land-surface drivers and thus in evaporation, and

3. discovering which regions are affected by the Atlantic modes, by ENSO, and where the impacts of the modes overlap.

2 Data

This study uses satellite-based and a reanalysis datasets Satellite-based datasets have strengths but also limitations, for example, in measuring soil moisture over densely forested canopies (Beck et al., 2021); errors in the root zone compromise the estimation of plant water stress and, thus, the skill of the evaporation estimate. On the other hand, simulations of evaporation which ingest reanalysis outputs might inherit their biases (Gebrechorkos et al., 2024; Valencia et al., 2023). Although the performance of both data sources has improved in recent years (Beck et al., 2021; Xie et al., 2024), their estimates remain uncertain, and confidence in their inter-annual dynamics rests on the fact that the analysed signals are evident in independent datasets. Therefore, we look for consistency in the dynamics of both sources of information.

2.1 Reanalysis

The ECMWF ERA5 reanalysis provides information on atmospheric variables that influence the evapotranspiration drivers and also related to the dynamics of the coupled ocean-atmospheric modes (Hersbach et al., 2020). Monthly time series of winds, vertically Integrated water vapour Flux (VIMF), mean SLP and vertically integrated moisture flux divergence (MDiv) are taken from it ERA5-Land is a land-surface simulation operationally forced by ERA5 which includes detailed modules on: infiltration, four-layer physically-based soil water storage, plant water-uptake, phenology and transpiration, and evaporation from soil and canopy interception (Muñoz-Sabater et al., 2021; ECMWF, 2023). From it, we download or derive the net surface Radiation (Rn), the volumetric soil water content in the first soil layer (hereafter soil moisture - SM) and the total evaporation (hereafter also referred to as evapotranspiration - ET).

2.2 Satellite

Precipitation is associated with moisture convergence; thus, satellite-based rainfall anomalies might be consistent with reanalysed MDiv anomalies. This research uses two precipitation products: the Multi-Source Weighted-Ensemble Precipitation v2.8

(MSWEP)(Beck et al., 2019) and the Climate Hazard group InfraRed Precipitation with Stations (CHIRPS)(Funk et al., 2015).
Both datasets are created with gauge and satellite data but differ in their sources. MSWEP also uses ERA5 rainfall estimates
80 but strongly in the extra-tropics whereas satellite data is given stronger weights in the tropics.

Three satellite-based datasets complement the three ERA5-Land variables: the European Space Agency Climate Change
Initiative for Soil Moisture v08.1 (ESI-CCI-SM) (Gruber et al., 2019), the total evaporation from the Global Land Evaporation
Amsterdam Model v3.8a (GLEAM) (Martens et al., 2017), and the EUMETSAT CLARA-A3 cloud area fraction as a proxy of
net radiation (Karlsson et al., 2023). GLEAM uses a three-layer conceptual root zone soil module from which vegetation can
85 access water (which considers ESA-CCI-SM assimilation where available). It includes a module for plant stress based on SM
and vegetation phenology, and it also provides evaporation from interception and bare soil. GLEAM uses ERA5 radiation as
forcing.

We use Sea Surface Temperature Anomalies (SSTAs) from the Extended Reconstructed SST version 5 (Huang et al., 2017)
– which is used as the primary dataset – and the Hadley Center Sea Ice and SST version 4.0.1 Kennedy et al. (2019). The
90 datasets are used to identify the ocean-atmospheric modes that had an impact on the analysed region and to define their active
phases.

3 Methods

3.1 Location and seasonal changes of ET drivers

This study explores two main evaporation drivers to afterwards search for the ocean-atmospheric modes that control those
95 drivers. SM and net radiation are classified with a multi-linear regression slope, using their seasonally standardised anomalies
targeting those of evapotranspiration. This analysis can suggest whether the evaporation anomalies are associated with water
availability or a radiation anomaly (evaporation regime).

3.2 Composites

This study uses composite analysis to exemplify the state of the atmosphere and the land surface at the active phase of the
100 Atlantic modes. All datasets are used between Dec-1979 and Nov-2020, aggregated at seasonal scale and analysed for each
season individually and synchronously.

Coupled ocean-atmospheric modes are identified with SSTA indices. The SSTA are first detrended to exclude the effect
of climate change from the analysis using a regression with de-seasonalised CO_2 ($R^2 = 0.92$, $p < 0.001$) (Thoning et al.,
1989); the CO_2 concentration is used to consider its continuous change in the XX century and to avoid subtracting the internal
105 variability. We performed Principal Components Analysis over the detrended SSTA and the resulting loadings were contrasted
with the literature review (Fernandes et al., 2015; Vallès-Casanova et al., 2020; Ruiz-Barradas et al., 2000)(supplementary
Figure S6). Correlation analysis between the principal components and hydrological variables indicated which modes have an
impact on South America (not shown). Therefore, we define the modes indices based on SSTA area-average boxes similar to

the principal component loadings of the Atlantic SSTs (Figure S6). The AMM monthly index is defined as the subtraction of
110 spatially averaged tropical southern Atlantic SSTA [40°W-0°W]x[25°S-5°S] from the northern domain [70°W-15°W]x[5°N-
25°N]; the Atl3 monthly index is identified as the spatial average of eastern tropical Atlantic SSTAs [20°W-0°]x[3°S-3°N].

To define the composite time steps, each mode's phase is established based on the indices. The positive and negative phases
are identified when their indices are above or below ±1 standard deviation, respectively, and otherwise are defined as neutral
phase (threshold for mode's activation); the latter is defined with the individual seasonal distributions (indices time series in
115 Figure S6). The asymmetric impacts of the modes are assessed by adding both extreme phases (positive plus negative), allowing
the recognition of the different impacts exerted by each phase. The composite's statistical significance is assessed with the two-
sample Student's two-tailed T-test, testing positive or negative phase against the neutral. Regarding precipitation, half of the
cell's time series have skewed distributions (Shapiro-Wilk test; not shown); thus, the Mann-Whitney U test is instead used. We
did not find a significant correlation of evapotranspiration with CO_2; nevertheless, evaporation time series are detrended with
120 a linear trend to also exclude global warming (Zhang et al., 2016), before being used in the composites.

ENSO develops in the second semester and its peak season is DJF. On the other hand, the AMM is more active from February
onwards but might last until SON (Yoon and Zeng, 2010); the Atl3 is more active in JJA (Vallès-Casanova et al., 2020). In DJF,
the AMM-associated anomalies are evident over the Atlantic but its effect over the continent is diluted (not shown). Therefore,
we analyse the influence of the Atlantic modes from March to September.

3.3 Conjoint effect with ENSO

We also perform grid-wise partial correlation analysis between the two Atlantic indices, the El Niño Longitude Index (ELI)(Williams
and Patricola, 2018), with evapotranspiration. The ELI considers the type of ENSO event (east or central Pacific). The purpose
of this analysis is to find those regions that are driven by an Atlantic mode but might also have impacts from another mode
when it is also active (i.e. simultaneously controlling the analysis by the effect of ENSO and the other Atlantic mode).

4 Results

4.1 Key evapotranspiration drivers

The classification of ET regime follows the migration of the Intertropical Convergence Zone (ITCZ, located in the south
Amazon in DJF and over north Orinoco in JJA)(Fig. 1). Panels a to d in Figure 1 show that the majority of ET variance can
be explained by just considering SM and radiation, with some exceptions where wind speed or vapour pressure deficit might
135 be important. MAM, the north-easterly winds bring moisture from the Atlantic and produce convergence and rainfall over
the Amazon in such an amount that the soil saturates, giving the conditions for an energy-limited evaporation. However, the
north of the Orinoco basin still behaves as a water-limited environment. As the ITCZ moves northward in JJA, the rainfall
recharges SM, changing Orinoco's behaviour to energy-limited, whereas other regions transform from energy- to water-limited
regimes like Northeast Brazil, as well as the south Amazon. The core of the Amazon rainforest still acts as energy-limited
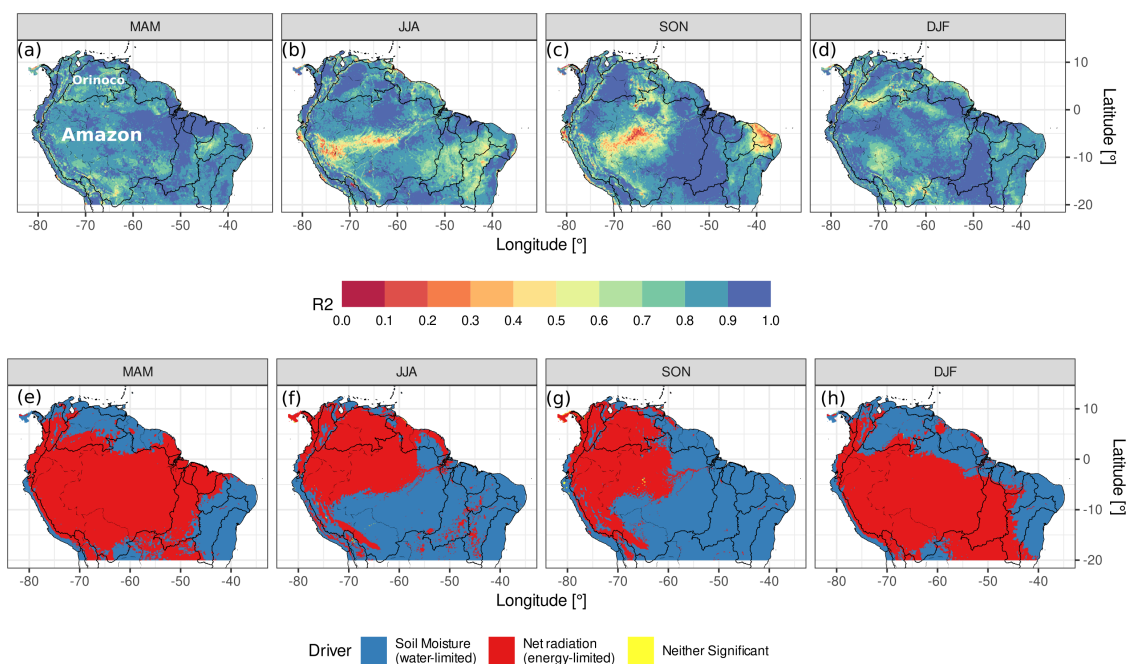
Figure 1. Classification of ERA5-Land evapotranspiration driver based on regression coefficients for each season. (a-d) Adjusted coefficients of determination for the multiple regression of SM and Rn standardised anomalies targeting those of ET and (e-h) variable with the highest significant coefficient. Panels are divided by the seasons (a,e) for MAM, (b,f) for JJA, (c,g) for SON and (d,h) for DJF. Black lines delineate the major river basins in South America, same boundaries used in the following figures.

(the latter region is energy-limited throughout the year). In SON, the ITCZ begins to move southward, but the energy-limited regime is concentrated in the west of the Amazon; the east and southeast basins are still on a water-limited regime. The Orinoco still behaves as energy-limited even though this is the transition season from wet to dry. In DJF, the evaporation in the south Amazon will depend on the available energy as the ITCZ is on its southern continental location; above-average radiation would produce more evaporation. The energy-limited regions correspond to those where SM is above the soil's field capacity (ECMWF, 2023)(not shown), and not all the continent is primarily driven by variations in energy supply.

The interactions between SM availability, plant water uptake and radiation lead – in some cases – to above-average evapotranspiration during negative precipitation anomalies (reduced moisture convergence and clouds). This behaviour is present in energy-limited regimes, whereas in water-limited environments negative moisture convergence anomalies bring less rainfall and cause below-average evapotranspiration.

4.2 Chain between the Atlantic modes and the evapotranspiration

The interannual variability of atmospheric circulation affects the key climatic drivers of evapotranspiration. Hence, circulation anomalies will impact evapotranspiration through a chain of events starting with: atmospheric moisture transport anomalies

(VIMF); which changes moisture flux divergence (MDiv), cloud formation and radiation availability; which simultaneously impacts precipitation and then Soil Moisture; and afterwards impact evapotranspiration. The steps in the chain repeat as far as

155 a mode is active; however, the impacts have important geographical differences depending on the season analysed.

4.2.1 March - May (MAM) Austral Autumn

The Atlantic Meridional Mode (AMM) consists of an SST and SLP seesaw between the Tropical North and South Atlantic, creating cross-equatorial wind anomalies (see Figure S1 for SLP and 850 hPa winds composites). In austral autumn, the positive phase redirects and advects moist air northward, towards the Orinoco, where it provokes positive convergence and precipitation

160 anomalies (Fig. 2a). The location of the satellite precipitation and reanalysed convergence anomalies are consistent between both datasets. Soil Moisture (SM) is impacted by the anomalous rainfall, Figure 2d and f shows that SM anomalies in northern Orinoco are sensitive to the AMM in positive phase; ESA-CCI-SM is available for this region and shows similar dynamics (Fig. S2). The western and southern Amazon have SM anomalies lower than absolute 2% as it is the rainy season and the soil is near saturation.

165 The evapotranspiration is afterwards impacted. The Orinoco behaves as water-limited (Fig. 1e) as this is the transition from dry to wet season, then the increase in rainfall and SM causes above-average evaporation (Fig. 2g). Over northeast Brazil, the positive phase produces divergence anomalies and less cloud cover (Fig. 2a; S4 for correlations with cloud cover). The latter increases net surface radiation but drives higher evapotranspiration than average due to the high SM availability above the soil's field capacity which allow the region to act as energy-limited (Fig. 1e and 2g). GLEAM independently shows similar results

170 over north Orinoco – more extended increase in evaporation – but over northeast Brazil the region with increased evaporation is smaller than in ERA5-Land and is surrounded by negative anomalies (Fig. S3).

In the negative phase, the AMM redirects the VIMF southward towards Northeast Brazil (Fig. 2b). The latter generates greater convergence, which reduces radiation and then evaporation over that region (Fig. 2b,e and h). Over the north Orinoco, the southward moist advection causes a reduction in rainfall and below-average SM, further limiting evaporation. The eastern

175 Amazon evaporation is not affected as in the positive phase (asymmetry). However, GLEAM estimates show that in northeast Brazil the impacted area is not as big as in ERA5-Land and do not show evaporation anomalies where the ESA-CCI-SM was unable to detect values (Fig. S2 and S3).

Comparing positive and negative phases, the mode shows asymmetric atmospheric circulation, with the negative phase being stronger in magnitude for the VIMF (Figure S5). The latter causes a decrease in SM over the northeast Amazon that is higher

180 than the increase in the positive phase, considering absolute values. Regarding evaporation, some regions are just affected in one phase of the mode such as the eastern Amazon and its river delta.

4.2.2 June - July (JJA) Austral Winter

In JJA, the Atlantic Meridional Mode (AMM) positive phase redirects the VIMF anomalies northward. This enhances convergence over the Caribbean and the divergence over the central Amazon and southern Orinoco (the latter having enhanced

185 convergence in the previous season); hence, it reduces clouds and rainfall over the continent (Figure 3a and c). The SM levels
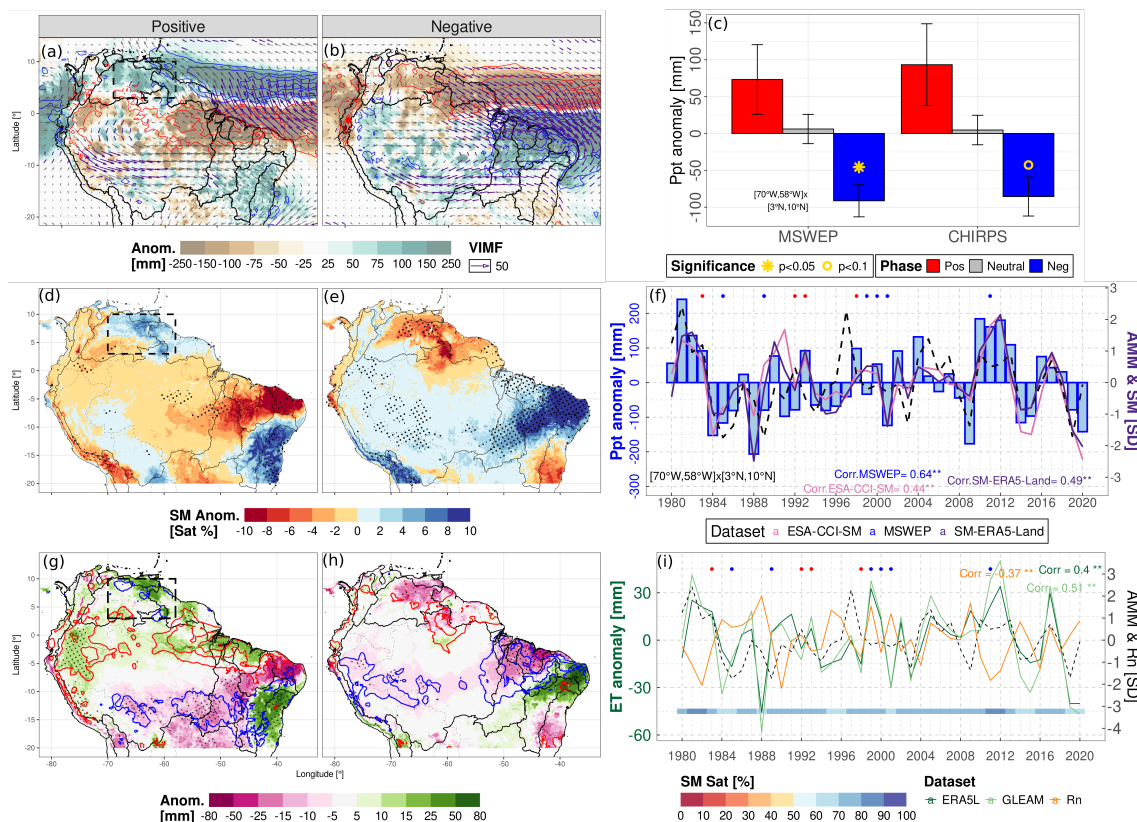
Figure 2. For Austral Autumn - MAM, composites of AMM for (a) VIMF (arrows), MDiv (contours) and MSWEP precipitation (shading) anomalies in the positive; positive MDiv anomalies are in red and negative in blue every 3 kg/m^2, precipitation is in mm and VIMF in kg/m/s. VIMF is depicted in purple arrows when the difference with the neutral phase is statistically significant at a 90% confidence level and in grey otherwise. (b) The same as (a) but for the negative phase. (c) Average precipitation anomalies inside the rectangles drawn in panel (a), for the three phases of the phenomena (Positive, Neutral and Negative). Whiskers show the composites' standard error and the gold symbols the significance level. (d) Composites of ERA5-Land SM saturation percentage anomalies in the AMM positive phase; black stipple dots depict regions where the difference with the neutral phase is statistically significant at a 95% confidence level. (e) same as (d) but for the negative phase. (f) Area-average MSWEP precipitation (bars) and SM standardised anomalies time series (lines) for the same boxes in panel (d); the Atlantic index time series is in black dashed lines in standard deviation and top points show ENSO active periods, positive phase in red and negative in blue. Pearson correlations are calculated with the respective Atlantic index, 95% confidence level is indicated with **. (g) Composites of ERA5-Land evapotranspiration (shadings) and net surface radiation anomalies (contours) in the AMM positive phase; positive radiation anomalies are in red and negative in blue every 3 W/m^2. (h) same as (f) but for the negative phase. (i) Area-average evapotranspiration time series (greens), ERA5-Land net surface radiation (orange), standardise Atlantic index (black dashed) and ERA5-Land SM in saturation percentage at the bottom of the panel with coloured rectangles. Boxed region: North Orinoco.

guarantee an energy-limited environment in the northern Amazon (Fig. 1f), and the AMM-related divergence generates above-average radiation, causing higher than average evaporation in the tropical forest (Fig. 3g). In the southern area, the dry season
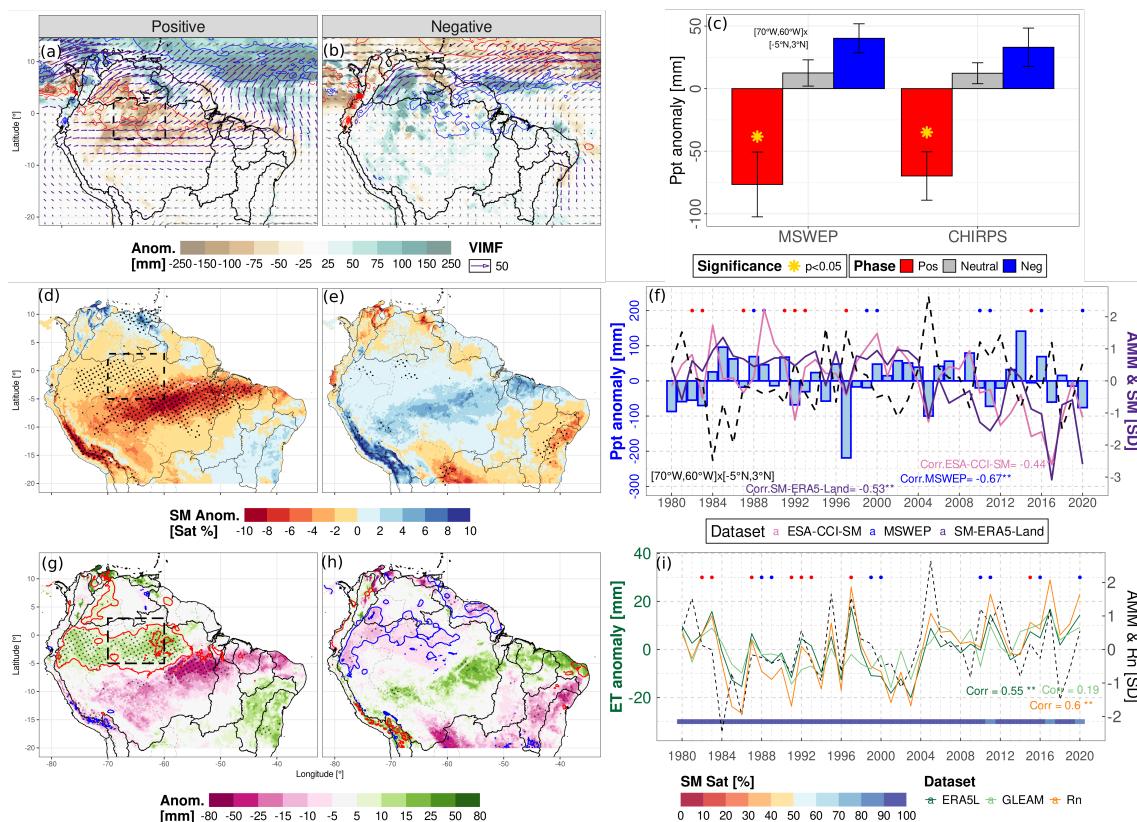
Figure 3. As in Figure 2 but for the Atlantic Meridional Mode (AMM) in June to August (JJA). Boxed region: Central Amazon.

and below-average SM cause trees to uptake water probably just through their deep roots generating water stress and reduced evaporation (see Sect. 5 Discussion). However, GLEAM estimates do not show any significant anomaly in the Amazon where
190 the availability of ESA-CCI-SM estimates are scarce (see time series and correlations in Figure 3f and i, and Fig. S2 and S3); both datasets show similar anomalies over the north coast.

In the negative phase, southward moisture flux brings more rainfall to the Orinoco but it is not clear over the Amazon, asymmetric condition (Fig. S5). Then, the AMM negative phase produces positive but not significant SM and evaporation anomalies in the southeast (Fig. 3e and h), although ERA5 suggest enhanced convergence not consistent in the rainfall datasets
195 (Fig. 3b and c). An important difference comparing JJA to MAM is the westward migration of the divergence anomalies from northeast Brazil to central Amazon and the effects on SM and evaporation.

Regarding the Atlantic El Niño (Atl3), it is characterised by a decrease in SLP and an increase in SST over the equatorial east Atlantic (Fig. S1). It typically peaks in JJA and weakens the trade winds through Bjerknes feedback with effects over the continent. The Atl3 impacts are not clear in other seasons (SON and DJF), when the AMM and ENSO exert a more discernible
200 influence (not shown). Figure 4a shows the westerly VIMF anomalies over the Guianas, producing convergence and significant
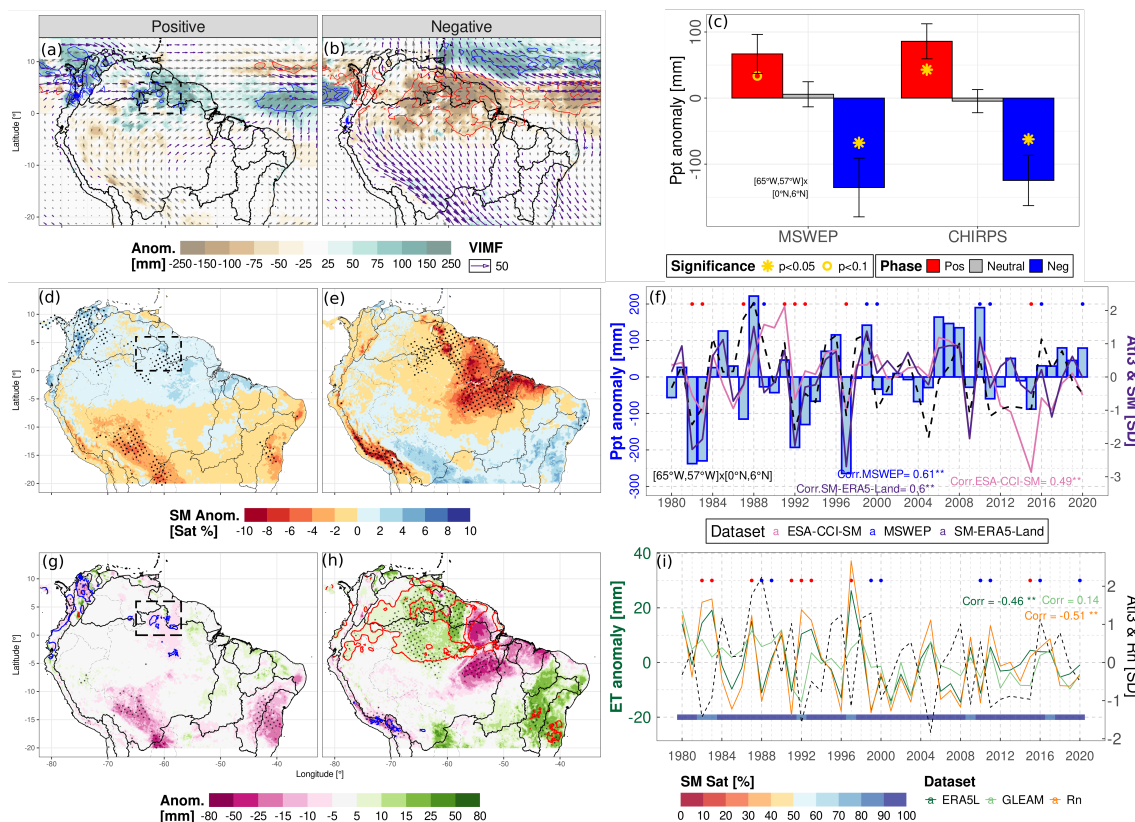
Figure 4. As in Figure 2 but for the Atlantic El Niño (Atl3) in June to August (JJA). Boxed region: North Amazon and Guianas.

positive precipitation anomalies (Fig. 4c). SM and evaporation are not extensively impacted by the Atl3 as changes in radiation are barely visible (Fig. 4d and g).

Conversely, stronger JJA trade winds increase Ekman pumping and mixing over the Atlantic and manifest as colder SST (known as Atlantic La Niña – Atl3 negative phase). The strengthened easterly winds – and VIMF – create negative anomalies of convergence and precipitation in an extended region over the East. However, greater MDiv and radiation increase evaporation over the east Orinoco and the Guianas due to the energy-limited environment, whereas over Northeast Brazil and the eastern Amazon the anomalies are negative as they behave as water-limited and the SM is also lower-than-average (Fig. 1f and 4e,h). GLEAM shows a similar but weak signal over the east Orinoco, Amazon delta and northeast Brazil (Fig. S3); ESA-CCI-SM is not available over the Guianas and partially over northeast Brazil. The negative phase is more pronounced due to stronger anomalies in all three variables (Figure S5 for asymmetric conditions). The evaporation between the two phases is very asymmetric as the eastern Orinoco and northeast Brazil are not affected in the positive phase but they are in the negative (Fig. 4g and h, and Fig. S5).

4.2.3   September - November (SON) Austral Spring

For this season, the AMM-related anomalies migrate to the western Orinoco and western Amazon since the rainfall is con-
centrated on the Andes' eastern slope. The reduction of VIMF and convergence in the positive phase leads to high radiation
anomalies that interact with the SM causing above-average evaporation over the Orinoco (5a, d and g). This is generated by
SM remaining high in the region, creating an energy-limited environment although it is not the core of the rainy season and the
SM anomalies are less than 2% (Fig. 1g and 5d and f). Moreover, the positive phase causes a decline in SM and ET over the
water-limited southeast due to the reduction of rainfall. There is no significant change in central northern Amazon, just in the
west or the east.

In the negative phase, the AMM brings extra moisture more strongly than the positive phase, although in both phases the
southeastern Amazon is impacted (Fig. 5a-c). In the latter region, the SM shows higher-than-average values, which grant the
land surface the extra moisture to increase evaporation in the water-limited zone (Fig. 5e-h). Over the Orinoco, the reduced
radiation causes less evaporation but also over the western and northern Amazon (the latter region not affected in the positive
phase, asymmetry Fig. S5). GLEAM shows similar results except for the central Amazon, again a region where the satellite
SM is not assimilated in the model (Fig. S2 and S3).

4.3   Atlantic modes connection with ENSO and impacts on evapotranspiration

Both ENSO and the Atlantic modes are connected through tropical and extra-tropical mechanisms, but each of them has effects
on South America's hydroclimate. The partial correlation shows a conjoint effect of ENSO and AMM over the evaporation
of northeast Brazil in austral autumn and in JJA (Fig. 6a,b,e,f), yet ENSO also impacts the eastern Amazon and the AMM
the Orinoco (see Sect. 5 Discussion). Whereas in SON, the AMM and ENSO tend to impact different regions (ENSO being
strong over the Guianas and the AMM over the west and southeast). The Atl3 does not show strong correlations and the ENSO
pattern for JJA is very similar to the Atl3 negative phase composites (Fig. 6b and h), indicating some overlapping dynamics
with ENSO probably related to the increased divergence and radiation. The impact of ENSO in DJF causes a reduction of
convergence and rainfall and increases radiation (Fig. 6d).

5   Discussion

Much of the research has focused on precipitation variability rather than on evapotranspiration (Arias et al., 2021; Marengo
and Espinoza, 2016; Poveda et al., 2006; Espinoza et al., 2011). Regarding evaporation, using machine learning Martens
et al. (2018) globally estimated the impacts of the AMM – and other modes –- finding the increased evapotranspiration over
Northeast Brazil in MAM and some cells in the central Amazon in JJA. However, our research focused on the modes that alter
the atmospheric circulation close to the continent and constitute the physical mechanism causing the teleconnection. Other
investigations focused specifically on ENSO's impact on Amazon evapotranspiration and SM (Moura et al., 2019; Poveda
et al., 2001). Specifically, Moura et al. (2019) show the anomalies of evapotranspiration for both south Amazon's rainy –
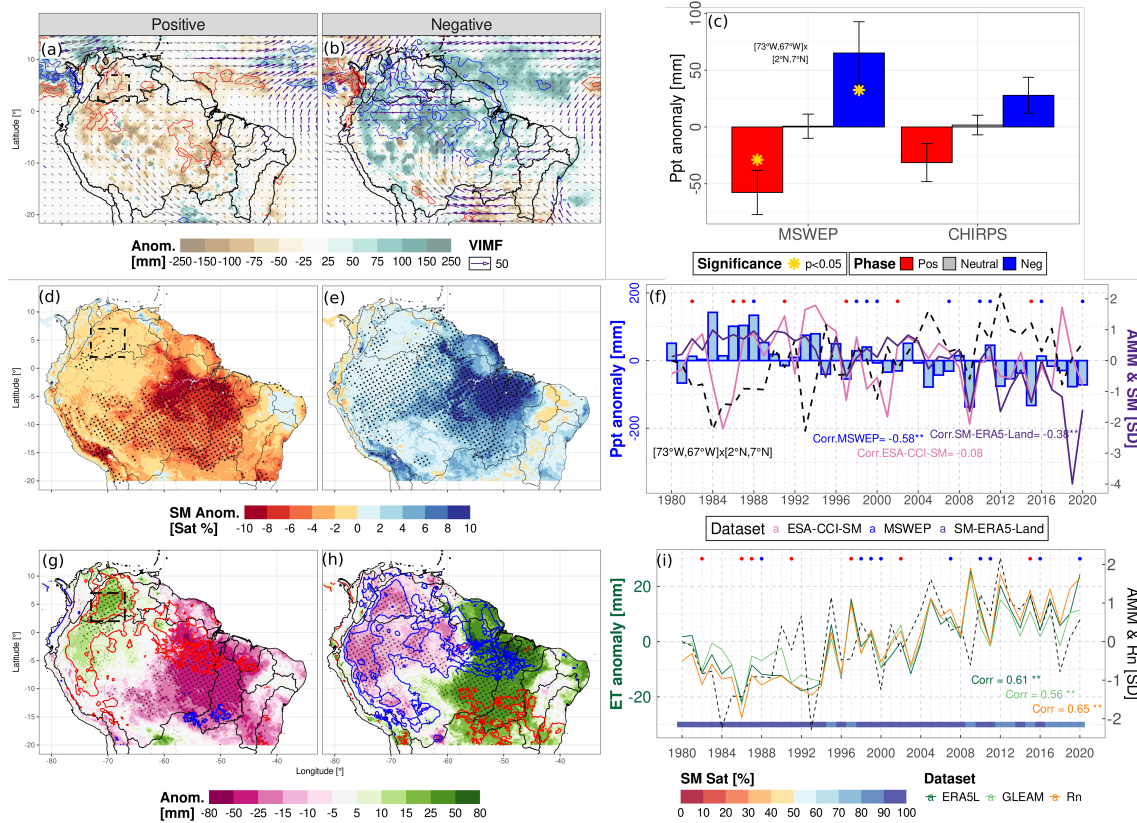
Figure 5. As in Figure 2 but for the Atlantic Meridional Mode (AMM) in September to November (SON). Boxed region: Western Orinoco.

DJF – and dry seasons during ENSO events, finding the increase in the evaporation also shown in our correlation analysis in
245 DJF. Our research focuses on the interaction between the atmosphere and the land surface, finding that the impacts migrate
from the eastern Amazon to the western Orinoco and that important asymmetries exist between phases. Hasler and Avissar
(2007) found an increase in evaporation in the equatorial Amazon during the dry season related to radiation anomalies, as
found in our ERA5-Land composites. The retained SM above critical values (soil's field capacity), up to the next season, might
cause positive evapotranspiration anomalies during below-average precipitation and above-average radiation periods (Zanin
250 et al., 2024); this is evident in our results in the transition from the wet to the dry season. The variability of evaporation has
implications for moisture-recycling, mainly for southeastern South America as pointed out by Drumond et al. (2014), and for
vegetation activity (Zhao et al., 2018).

Differences between GLEAM and ERA5-Land stem from their formulation structures and assimilated data, which are then
propagated to the composite analysis. The influence of wind speed on evapotranspiration is not considered in GLEAM v3.8, and
255 the soil module and plant physiology are more accurate in ERA5-Land. The impediment of assimilating SM due to the scarcity
of ESA-CCI-SM data in dense forest areas might compromise the uncertainty in GLEAM estimates (Baker et al., 2021), e.g.
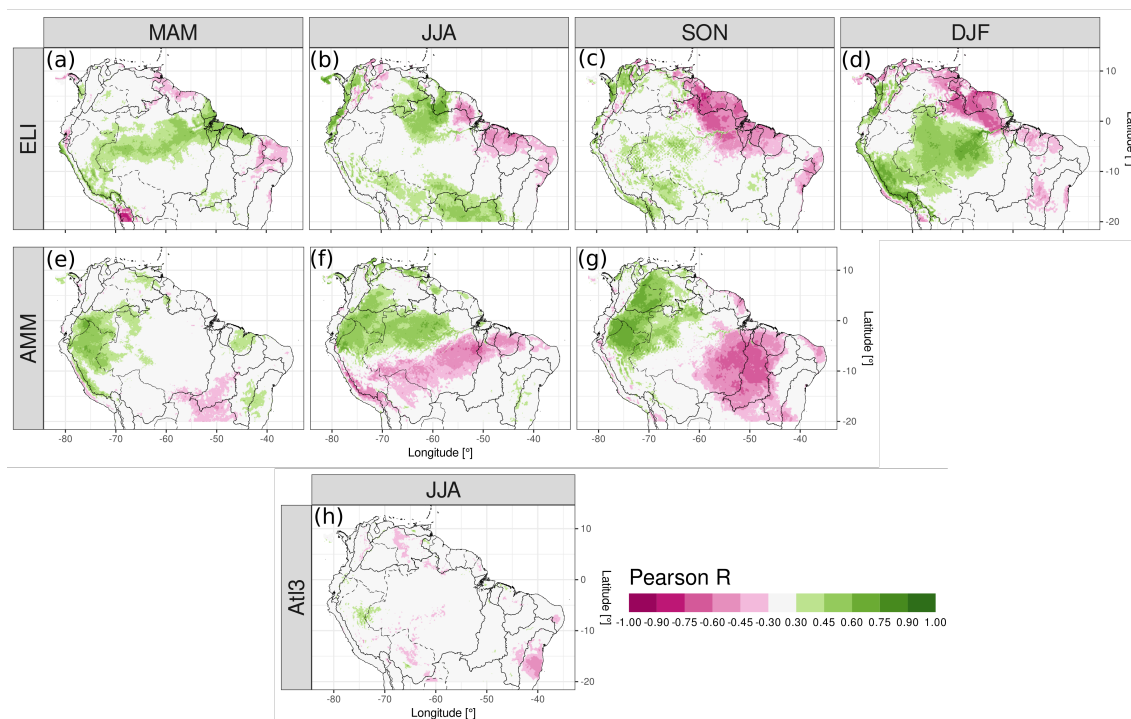
Figure 6. Partial correlation of ET from ERA5-Land with the main tropical ocean modes in the Atlantic and Pacific. Panels a-d are the correlations with ELI for each season, controlling by the two Atlantic indices, e-g are the correlations with the AMM except for DJF controlling by ELI and Atl3, and panel h is the correlation with the Atl3 controlling by ELI and the AMM. Just 95% confidence level values are shown in colours.

over the northern Amazon and Delta, and over the Guianas (Fig. 4d,e and 5d,e). Some studies have compared both datasets against eddy-covariance towers and water-balance approaches and concluded that ERA5-Land estimates are more realistic than GLEAM (Muñoz-Sabater et al., 2021; Xie et al., 2024). The bias in ERA5's rainfall might be diverted towards the streamflow
260 (Towner et al., 2021), rather than generating a bias on the SM and the evaporation. These limitations are probably the main cause of the differences between the composites using each dataset. In forested areas, roots deeper than 1.5 m allow the water uptake from deep layers as a survival mechanism (Roberts et al., 2005; O'Connor et al., 2019; Jarvis, 1976), their main driver of evaporation is most likely the incoming radiation but trees might still feel water stress (Lian et al., 2024). The latter is partially considered in ERA5-Land as the depth of the last layer is deeper than 1.5 m and plants withdraw soil moisture root-
265 percentage-wise (ECMWF, 2023), whereas in GLEAM the three soil layers depth is not specified and plants withdraw water from the wettest layers (Martens et al., 2017). D'Acunha et al. (2024) found low evaporation rates in cropland and pasture sites inside the southeast Amazon rainforest compared to natural land use; the structure of both datasets in our study considers the grasslands and the other land covers, with some limitations.

The AMM and the Atl3 are influenced by and also have feedback with ENSO (García-Serrano et al., 2017; Martín-Rey
et al., 2014; Cai et al., 2019). Our results show that each mode impacts different regions, except for northeast Brazil where
they overlap through El Niño enforcing convection inhibition and the AMM producing anomalous moisture advection (Chiang
et al., 2002); these mechanisms then modify convergence, rainfall, radiation availability and thus evaporation. The AMM
negative phase has been less recurrent in SON in the last decades associated with a positive phase of the Atlantic Multidecadal
Oscillation (AMO)(general interhemispheric temperature gradient) (Brönnimann et al., 2015; Friedman et al., 2020). The latter
is apparently related to the reduced aerosol forcing over the northern hemisphere and its associated radiation scattering (Hua
et al., 2019; He et al., 2023). The Atl3 negative phase has co-occurred with the ENSO positive phase (El Niño), which is
evident in our composites and partial correlation analysis. ENSO causes downward atmospheric movement over the east of the
Amazon that hampers convection and precipitation (Cai et al., 2020); simultaneously, the strengthened easterlies of the Atl3(-)
and the moisture divergence over the Guianas undermine precipitation. However, the relationship between ENSO and the Atl3
is inconsistent (Chang et al., 2006; Lübbecke and McPhaden, 2012).

Several ocean-atmospheric drivers have been identify to influence the hydrometeorology of South America. Rodrigues and
McPhaden (2014) analysed the AMM effects on precipitation in Northeast Brazil and the Amazon, while others focused
on the decadal variations of precipitation and streamflow or the low atmospheric dynamics (Fernandes et al., 2015; Lopes
et al., 2016; Olmo et al., 2022). Our research shows that the chain of events starting with the SSTA, and moving to VIMF,
MDiv and precipitation anomalies are linked to the variability of evaporation. However, we also show that the AMM also
affects the Orinoco basin in MAM, JJA and might even extend into SON (Yoon and Zeng, 2010), not just over the Amazon
and precipitation but also over the SM and the evapotranspiration. There is agreement in the comparison of the location of
reanalysed convergence and satellite precipitation; the rainfall anomalies influence peak river flow, and our results agree with
the location of peak river flow reduction during TNA anomalies reported by Towner et al. (2021) – decrease in central Amazon
in the positive phase. Regarding the Atl3, most of the studies have focused on its statistical relationship with continental
precipitation anomalies (Gu and Adler, 2009; Torralba et al., 2015), and the atmospheric dynamics of its development (Vallès-
Casanova et al., 2020).

Although coupled ocean-atmospheric modes are important drivers at seasonal time scale as shown here, other sources of
variability at other scales – such as those mentioned in Sect. 1 Introduction – influence precipitation and might also influence
evaporation (Mariotti et al., 2018). They might affect the transition and migration of the anomalies from one season to the
following one. Phenomenons with longer frequencies such as the AMO have also been discussed here, but the impacts of all
those sources deserve further research.

6 Conclusions

This research advances the current understanding of the physical mechanisms that cause the interannual climate and land-
surface variability in Tropical South America, focusing on soil moisture and evaporation. It elucidates the Atlantic SST modes'
influence on upwind conditions that impact the Orinoco basin and not just Northeast Brazil or the Amazon. Atlantic ocean-

atmospheric interactions drive moisture convergence anomalies, in turn modifying water and radiation availability, which then control the Soil Moisture and evaporation anomalies (chain of events).

The Atlantic El Niño weakens the trade winds in JJA producing convergence over the Guianas and eastern Orinoco. However,
305 its effect on the SM, radiation and evaporation is not strong. The negative phase – in conjunction with ENSO – strengthens the trade winds and produces divergence over an extended region which significantly changes the land-surface variables.

The AMM creates cross-equatorial SLP anomalies that deflect climatological winds not just over the ocean but also over the continent. It retrieves moisture northward on the positive phase, on occasions increasing and in others reducing convergence, precipitation and radiation depending on location and season, hence causing the land-surface anomalies. The negative phase
310 causes the contrary effect but with strong asymmetries. In MAM, the moisture is redirected towards the Orinoco – from northeast Brazil –, whereas in JJA and SON it is taken from south Orinoco and north Amazon (or brought to the same regions in the other phase with important differences in zonal direction). The changes in moisture transport depend on the annual wind pattern, producing different effects over the Orinoco when comparing MAM and JJA.

The regions impacted in each phase might be different. Analysing just one phase might lead to misleading estimations in
315 several variables.

Evapotranspiration is not only influenced in its regime by the ITCZ position but also by the phase of the ocean-atmospheric mode. This is related to the fact that SM is not resilient to the activation of the modes unless it is the rainy season when in whatever phase the soil is saturated; the SM saturation percentage closely varies with the ITCZ position. For instance, evapotranspiration anomalies in Northeast Brazil in MAM or in western Orinoco in SON are energy-limited but the sign of the
320 anomaly depends on the phase of the AMM. Examples of water-limited evaporation anomalies are North Orinoco in MAM and South Amazon in SON where the Atlantic mode brings more precipitation. The latter dynamic unfolds in the dry to wet transition season, the low SM level is affected but does not quickly or necessarily translate into more evapotranspiration (it depends on the phase of the mode). The analysed phenomena have implications for gross primary production, the carbon cycle and can be used for predicting the response of ecosystems' activity.

325 Our conclusions are underpinned by the consistency between independent observations of land-surface and atmospheric variables whose robustness comes from physically-based interpolations (reanalysis) or satellite-based observations. Limitations arise from the dataset's uncertainty and satellite retrievals; deforestation dynamics are also not included in the datasets. Nevertheless, the general circulation is still well represented due to the assimilation of atmospheric pressure, and models and measurements are as accurate as possible. Both sources of information show similar impacts but with local differences mostly
330 in dense forested areas where physically based models like ERA5-Land might be more reliable. Longer time series of eddy-covariance towers could help the community confirm the dynamics discovered in our study. All in all, the datasets are accurate enough to analyse interannual variability.

Code availability. We coded scripts in R (https://www.R-project.org/) to perform the analysis of the datasets. They can be consulted at: https://github.com/nduqueg/ET_var_SAme

335 *Data availability.* Extended Reconstructed SST version 5 (Huang et al., 2017) is available at: https://www.ncei.noaa.gov/pub/data/cmb/ersst/v5/netcdf/. Hadley Center Sea Ice and SST version 4.0.1 (Kennedy et al., 2019) is available at: https://www.metoffice.gov.uk/hadobs/hadsst4/data/download.html. Mauna Loa CO2 concentrations are available at https://gml.noaa.gov/ccgg/trends/data.html. ECMWF ERA5 reanalysis (Hersbach et al., 2020) and the ERA5-Land reanalysis (Muñoz-Sabater et al., 2021) data are available from Copernicus Climate Data Store web portal https://cds.climate.copernicus.eu. MSWEP (Beck et al., 2019) is available at: http://www.gloh2o.org/mswep/. CHIRPS

340 (Funk et al., 2015) is available at: https://data.chc.ucsb.edu/products/CHIRPS-2.0. ESA CCI SM (Gruber et al., 2019) is available at: https://catalogue.ceda.ac.uk/uuid/ff890589c21f4033803aa550f52c980c. GLEAM (Martens et al., 2017) is available at: https://www.gleam.eu/. EUMETSAT CLARA-A3 (Karlsson et al., 2023) is available at: https://wui.cmsaf.eu/safira/action/viewProduktDetails?fid=40&eid=22277_22492. HydroSHEDS basins are available at: https://www.hydrosheds.org/products/hydrobasins (Lehner and Grill, 2013)

Author contributions. Conceptualization: N.D-G and S.B.; Data Curation: N.D-G, A.R.F.; Formal Analysis: N.D-G; Funding Acquisition:
345 N.D-G, S.B.; Investigation:N.D-G, A.R.F, S.B.; Methodology: N.D-G, A.R.F., S.B.; Project Administration: N.D-G., S.B.; Resources: S.B.; Software: N.D-G; Supervision: S.B.; Validation: N.D-G, A.R.F., S.B.; Visualisation: N.D-G; Writing - original draft: N.D-G; Writing - review and editing: N.D-G, A.R.F., S.B.

Competing interests. The authors declare that they have no conflict of interest.

Acknowledgements. N.D-G. was supported by the Federal Commission for Scholarships for Foreign Students through the Swiss Government
350 Excellence Scholarship (ESKAS No. 2022.0563) for the academic year(s) 2022-2024. A.R.F. was funded by the European Union's Horizon 2020 research and innovation program under the Marie Skłodowska-Curie grant No. 894064 (AQUATIC). We are grateful with the institutions that gather and freely disseminate the data used in this research, and to Sonia Dupuis and Noemi Imfeld for recommending the names of some remote sensed products. N.D-G thanks Helena Gardeazabal, Joaquin Duque and friends for the emotional support throughout this research.

References

355   Arias, P. A., Martínez, J. A., and Vieira, S. C.: Moisture sources to the 2010–2012 anomalous wet season in northern South America, Climate Dynamics, 45, 2861–2884, https://doi.org/10.1007/s00382-015-2511-7, 2015.

Arias, P. A., Martínez, J. A., Mejía, J. D., Pazos, M. J., Espinoza, J. C., and Wongchuig-Correa, S.: Changes in Normalized Difference Vegetation Index in the Orinoco and Amazon River Basins: Links to Tropical Atlantic Surface Temperatures, Journal of Climate, 33, 8537–8559, https://doi.org/10.1175/JCLI-D-19-0696.1, 2020.

360   Arias, P. A., Garreaud, R., Poveda, G., Espinoza, J. C., Molina-Carpio, J., Masiokas, M., Viale, M., Scaff, L., and van Oevelen, P. J.: Hydroclimate of the Andes Part II: Hydroclimate Variability and Sub-Continental Patterns, Frontiers in Earth Science, 8, 1–25, https://doi.org/10.3389/feart.2020.505467, 2021.

Baker, J. C., Garcia-Carreras, L., Gloor, M., Marsham, J. H., Buermann, W., Da Rocha, H. R., Nobre, A. D., De Carioca Araujo, A., and Spracklen, D. V.: Evapotranspiration in the Amazon: Spatial patterns, seasonality, and recent trends in observations, reanalysis, and climate

365   models, Hydrology and Earth System Sciences, 25, 2279–2300, https://doi.org/10.5194/hess-25-2279-2021, 2021.

Beck, H. E., Wood, E. F., Pan, M., Fisher, C. K., Miralles, D. G., van Dijk, A. I. J. M., McVicar, T. R., and Adler, R. F.: MSWEP V2 Global 3-Hourly 0.1° Precipitation: Methodology and Quantitative Assessment, Bulletin of the American Meteorological Society, 100, 473–500, https://doi.org/10.1175/BAMS-D-17-0138.1, 2019.

Beck, H. E., Pan, M., Miralles, D. G., Reichle, R. H., Dorigo, W. A., Hahn, S., Sheffield, J., Karthikeyan, L., Balsamo, G., Parinussa, R. M.,

370   van Dijk, A. I. J. M., Du, J., Kimball, J. S., Vergopolan, N., and Wood, E. F.: Evaluation of 18 satellite- and model-based soil moisture products using in situ measurements from 826 sensors, Hydrology and Earth System Sciences, 25, 17–40, https://doi.org/10.5194/hess-25-17-2021, 2021.

Brönnimann, S., Fischer, A. M., Rozanov, E., Poli, P., Compo, G. P., and Sardeshmukh, P. D.: Southward shift of the northern tropical belt from 1945 to 1980, Nature Geoscience, 8, 969–974, https://doi.org/10.1038/ngeo2568, 2015.

375   Cai, W., Wu, L., Lengaigne, M., Li, T., McGregor, S., Kug, J. S., Yu, J. Y., Stuecker, M. F., Santoso, A., Li, X., Ham, Y. G., Chikamoto, Y., Ng, B., McPhaden, M. J., Du, Y., Dommenget, D., Jia, F., Kajtar, J. B., Keenlyside, N., Lin, X., Luo, J. J., Martín-Rey, M., Ruprich-Robert, Y., Wang, G., Xie, S. P., Yang, Y., Kang, S. M., Choi, J. Y., Gan, B., Kim, G. I., Kim, C. E., Kim, S., Kim, J. H., and Chang, P.: Pantropical climate interactions, Science, 363, https://doi.org/10.1126/science.aav4236, 2019.

Cai, W., McPhaden, M. J., Grimm, A. M., Rodrigues, R. R., Taschetto, A. S., Garreaud, R. D., Dewitte, B., Poveda, G., Ham, Y. G., Santoso,

380   A., Ng, B., Anderson, W., Wang, G., Geng, T., Jo, H. S., Marengo, J. A., Alves, L. M., Osman, M., Li, S., Wu, L., Karamperidou, C., Takahashi, K., and Vera, C.: Climate impacts of the El Niño–Southern Oscillation on South America, Nature Reviews Earth and Environment, 1, 215–231, https://doi.org/10.1038/s43017-020-0040-3, 2020.

Chang, P., Fang, Y., Saravanan, R., Ji, L., and Seidel, H.: The cause of the fragile relationship between the Pacific El Nĩo and the Atlantic Nĩo, Nature, 443, 324–328, https://doi.org/10.1038/nature05053, 2006.

385   Chiang, J. C., Kushnir, Y., and Giannini, A.: Deconstructing Atlantic Intertropical Convergence Zone variability: Influence of the local cross-equatorial sea surface temperature gradient and remote forcing from the Eastern Equatorial Pacific, Journal of Geophysical Research Atmospheres, 107, https://doi.org/10.1029/2000jd000307, 2002.

Compo, G. P. and Sardeshmukh, P. D.: Removing ENSO-related variations from the climate record, Journal of Climate, 23, 1957–1978, https://doi.org/10.1175/2009JCLI2735.1, 2010.

390 D'Acunha, B., Dalmagro, H., Zanella de Arruda, P., Biudes, M., Lathuillière, M., Uribe, M., Couto, E., Brando, P., Vourlitis, G., and Johnson, M.: Changes in evapotranspiration, transpiration and evaporation across natural and managed landscapes in the Amazon, Cerrado and Pantanal biomes, Agricultural and Forest Meteorology, 346, 109 875, https://doi.org/10.1016/j.agrformet.2023.109875, 2024.

Drumond, A., Marengo, J., Ambrizzi, T., Nieto, R., Moreira, L., and Gimeno, L.: The role of the Amazon Basin moisture in the atmospheric branch of the hydrological cycle: A Lagrangian analysis, Hydrology and Earth System Sciences, 18, 2577–2598,
395 https://doi.org/10.5194/hess-18-2577-2014, 2014.

ECMWF: IFS Documentation CY48R1 - Part IV: Physical Processes, in: IFS Documentation CY48R1, https://doi.org/10.21957/02054f0fbf, 2023.

Enfield, D. B.: Relationships of inter-American rainfall to tropical Atlantic and Pacific SST variability, Geophysical Research Letters, 23, 3305–3308, https://doi.org/10.1029/96GL03231, 1996.

400 Espinoza, J. C., Ronchail, J., Guyot, J. L., Junquas, C., Vauchel, P., Lavado, W., Drapeau, G., and Pombosa, R.: Climate variability and extreme drought in the upper Solimões River (western Amazon Basin): Understanding the exceptional 2010 drought, Geophysical Research Letters, 38, n/a–n/a, https://doi.org/10.1029/2011GL047862, 2011.

Fernandes, K., Giannini, A., Verchot, L., Baethgen, W., and Pinedo-Vasquez, M.: Decadal covariability of Atlantic SSTs and western Amazon dry-season hydroclimate in observations and CMIP5 simulations, Geophysical Research Letters, 42, 6793–6801,
405 https://doi.org/10.1002/2015GL063911, 2015.

Friedman, A. R., Hegerl, G. C., Schurer, A. P., Lee, S. Y., Kong, W., Cheng, W., and Chiang, J. C.: Forced and unforced decadal behavior of the interhemispheric SST contrast during the instrumental period (1881–2012): Contextualizing the late 1960s–early 1970s shift, Journal of Climate, 33, 3487–3509, https://doi.org/10.1175/JCLI-D-19-0102.1, 2020.

Funk, C., Peterson, P., Landsfeld, M., Pedreros, D., Verdin, J., Shukla, S., Husak, G., Rowland, J., Harrison, L., Hoell, A., and Michaelsen, J.:
410 The climate hazards infrared precipitation with stations—a new environmental record for monitoring extremes, Scientific Data, 2, 150 066, https://doi.org/10.1038/sdata.2015.66, 2015.

García-Serrano, J., Cassou, C., Douville, H., Giannini, A., and Doblas-Reyes, F. J.: Revisiting the ENSO teleconnection to the tropical North Atlantic, Journal of Climate, 30, 6945–6957, https://doi.org/10.1175/JCLI-D-16-0641.1, 2017.

Garreaud, R. D., Vuille, M., Compagnucci, R., and Marengo, J.: Present-day South American climate, Palaeogeography, Palaeoclimatology,
415 Palaeoecology, 281, 180–195, https://doi.org/10.1016/j.palaeo.2007.10.032, 2009.

Gebrechorkos, S. H., Leyland, J., Dadson, S. J., Cohen, S., Slater, L., Wortmann, M., Ashworth, P. J., Bennett, G. L., Boothroyd, R., Cloke, H., Delorme, P., Griffith, H., Hardy, R., Hawker, L., McLelland, S., Neal, J., Nicholas, A., Tatem, A. J., Vahidi, E., Liu, Y., Sheffield, J., Parsons, D. R., and Darby, S. E.: Global-scale evaluation of precipitation datasets for hydrological modelling, Hydrology and Earth System Sciences, 28, 3099–3118, https://doi.org/10.5194/hess-28-3099-2024, 2024.

420 Grimm, A. M. and Zilli, M. T.: Interannual variability and seasonal evolution of summer monsoon rainfall in South America, Journal of Climate, 22, 2257–2275, https://doi.org/10.1175/2008JCLI2345.1, 2009.

Gruber, A., Scanlon, T., van der Schalie, R., Wagner, W., and Dorigo, W.: Evolution of the ESA CCI Soil Moisture climate data records and their underlying merging methodology, Earth System Science Data, 11, 717–739, https://doi.org/10.5194/essd-11-717-2019, 2019.

Gu, G. and Adler, R. F.: Interannual variability of boreal summer rainfall in the equatorial Atlantic, International Journal of Climatology, 29,
425 175–184, https://doi.org/10.1002/joc.1724, 2009.

Hasler, N. and Avissar, R.: What Controls Evapotranspiration in the Amazon Basin?, Journal of Hydrometeorology, 8, 380–395, https://doi.org/10.1175/JHM587.1, 2007.

He, C., Clement, A. C., Kramer, S. M., Cane, M. A., Klavans, J. M., Fenske, T. M., and Murphy, L. N.: Tropical Atlantic multidecadal variability is dominated by external forcing, Nature, 622, https://doi.org/10.1038/s41586-023-06489-4, 2023.

430 Hersbach, H., Bell, B., Berrisford, P., Hirahara, S., Horányi, A., Muñoz-Sabater, J., Nicolas, J., Peubey, C., Radu, R., Schepers, D., Simmons, A., Soci, C., Abdalla, S., Abellan, X., Balsamo, G., Bechtold, P., Biavati, G., Bidlot, J., Bonavita, M., De Chiara, G., Dahlgren, P., Dee, D., Diamantakis, M., Dragani, R., Flemming, J., Forbes, R., Fuentes, M., Geer, A., Haimberger, L., Healy, S., Hogan, R. J., Hólm, E., Janisková, M., Keeley, S., Laloyaux, P., Lopez, P., Lupu, C., Radnoti, G., de Rosnay, P., Rozum, I., Vamborg, F., Villaume, S., and Thépaut, J. N.: The ERA5 global reanalysis, Quarterly Journal of the Royal Meteorological Society, 146, 1999–2049,
435 https://doi.org/10.1002/qj.3803, 2020.

Hirschi, M., Mueller, B., Dorigo, W., and Seneviratne, S. I.: Using remotely sensed soil moisture for land-atmosphere coupling diagnostics: The role of surface vs. root-zone soil moisture variability, Remote Sensing of Environment, 154, 246–252, https://doi.org/10.1016/j.rse.2014.08.030, 2014.

Hoyos, I., Cañón-Barriga, J., Arenas-Suárez, T., Dominguez, F., and Rodríguez, B. A.: Variability of regional atmospheric moisture over
440 Northern South America: patterns and underlying phenomena, Climate Dynamics, 52, 893–911, https://doi.org/10.1007/s00382-018-4172-9, 2019.

Hua, W., Dai, A., Zhou, L., Qin, M., and Chen, H.: An Externally Forced Decadal Rainfall Seesaw Pattern Over the Sahel and Southeast Amazon, Geophysical Research Letters, 46, 923–932, https://doi.org/10.1029/2018GL081406, 2019.

Huang, B., Thorne, P. W., Banzon, V. F., Boyer, T., Chepurin, G., Lawrimore, J. H., Menne, M. J., Smith, T. M., Vose, R. S., and Zhang,
445 H. M.: Extended reconstructed Sea surface temperature, Version 5 (ERSSTv5): Upgrades, validations, and intercomparisons, Journal of Climate, 30, 8179–8205, https://doi.org/10.1175/JCLI-D-16-0836.1, 2017.

IPCC: Climate Change 2021: The Physical Science Basis, Cambridge University Press, Cambriedge, United Kingdom, https://doi.org/10.1017/9781009157896, 2021.

Jarvis, P.: The interpretation of the variations in leaf water potential and stomatal conductance found in canopies in the field, Philosophical
450 Transactions of the Royal Society of London. B, Biological Sciences, 273, 593–610, https://doi.org/10.1098/rstb.1976.0035, 1976.

Karlsson, K.-G., Riihelä, A., Trentmann, J., Stengel, M., Solodovnik, I., Meirink, J. F., Devasthale, A., Jääskeläinen, E., Kallio-Myers, V., Eliasson, S., Benas, N., Johansson, E., Stein, D., Finkensieper, S., Håkansson, N., Akkermans, T., Clerbaux, N., Selbach, N., Marc, S., and Hollmann, R.: CLARA-A3: CM SAF cLoud, Albedo and surface RAdiation dataset from AVHRR data - Edition 3, https://doi.org/10.5676/EUM_SAF_CM/CLARA_AVHRR/V003, 2023.

455 Kennedy, J. J., Rayner, N. A., Atkinson, C. P., and Killick, R. E.: An Ensemble Data Set of Sea Surface Temperature Change From 1850: The Met Office Hadley Centre HadSST.4.0.0.0 Data Set, Journal of Geophysical Research: Atmospheres, 124, 7719–7763, https://doi.org/10.1029/2018JD029867, 2019.

Le, T. and Bae, D.-H.: Response of global evaporation to major climate modes in historical and future Coupled Model Intercomparison Project Phase 5 simulations, Hydrology and Earth System Sciences, 24, 1131–1143, https://doi.org/10.5194/hess-24-1131-2020, 2020.

460 Lehner, B. and Grill, G.: Global river hydrography and network routing: baseline data and new approaches to study the world's large river systems, Hydrological Processes, 27, 2171–2186, https://doi.org/10.1002/hyp.9740, 2013.

Lian, X., Morfopoulos, C., and Gentine, P.: Water deficit and storm disturbances co-regulate Amazon rainforest seasonality, Science Advances, 10, https://doi.org/10.1126/sciadv.adk5861, 2024.

Lopes, A. V., Chiang, J. C. H., Thompson, S. A., and Dracup, J. A.: Trend and uncertainty in spatial-temporal patterns of hydrological
465 droughts in the Amazon basin, Geophysical Research Letters, 43, 3307–3316, https://doi.org/10.1002/2016GL067738, 2016.

Lübbecke, J. F. and McPhaden, M. J.: On the Inconsistent Relationship between Pacific and Atlantic Niños, Journal of Climate, 25, 4294–4303, https://doi.org/10.1175/JCLI-D-11-00553.1, 2012.

Lübbecke, J. F., Rodríguez-Fonseca, B., Richter, I., Martín-Rey, M., Losada, T., Polo, I., and Keenlyside, N. S.: Equatorial Atlantic variability—Modes, mechanisms, and global teleconnections, Wiley Interdisciplinary Reviews: Climate Change, 9, 1–18, https://doi.org/10.1002/wcc.527, 2018.

Marengo, J. A. and Espinoza, J. C.: Extreme seasonal droughts and floods in Amazonia: Causes, trends and impacts, International Journal of Climatology, 36, 1033–1050, https://doi.org/10.1002/joc.4420, 2016.

Mariotti, A., Ruti, P. M., and Rixen, M.: Progress in subseasonal to seasonal prediction through a joint weather and climate community effort, npj Climate and Atmospheric Science, 1, 2–5, https://doi.org/10.1038/s41612-018-0014-z, 2018.

Martens, B., Miralles, D. G., Lievens, H., Van Der Schalie, R., De Jeu, R. A., Fernández-Prieto, D., Beck, H. E., Dorigo, W. A., and Verhoest, N. E.: GLEAM v3: Satellite-based land evaporation and root-zone soil moisture, Geoscientific Model Development, 10, 1903–1925, https://doi.org/10.5194/gmd-10-1903-2017, 2017.

Martens, B., Waegeman, W., Dorigo, W. A., Verhoest, N. E. C., and Miralles, D. G.: Terrestrial evaporation response to modes of climate variability, npj Climate and Atmospheric Science, 1, 43, https://doi.org/10.1038/s41612-018-0053-5, 2018.

Martín-Rey, M., Rodríguez-Fonseca, B., Polo, I., and Kucharski, F.: On the Atlantic–Pacific Niños connection: a multidecadal modulated mode, Climate Dynamics, 43, 3163–3178, https://doi.org/10.1007/s00382-014-2305-3, 2014.

Merz, B., Blöschl, G., Vorogushyn, S., Dottori, F., Aerts, J. C., Bates, P., Bertola, M., Kemter, M., Kreibich, H., Lall, U., and Macdonald, E.: Causes, impacts and patterns of disastrous river floods, Nature Reviews Earth and Environment, 2, 592–609, https://doi.org/10.1038/s43017-021-00195-3, 2021.

Miralles, D. G., Van Den Berg, M. J., Gash, J. H., Parinussa, R. M., De Jeu, R. A., Beck, H. E., Holmes, T. R., Jiménez, C., Verhoest, N. E., Dorigo, W. A., Teuling, A. J., and Johannes Dolman, A.: El Niño-La Niña cycle and recent trends in continental evaporation, Nature Climate Change, 4, 122–126, https://doi.org/10.1038/nclimate2068, 2014.

Mishra, A. K. and Singh, V. P.: A review of drought concepts, Journal of Hydrology, 391, 202–216, https://doi.org/10.1016/j.jhydrol.2010.07.012, 2010.

Moura, M. M., dos Santos, A. R., Pezzopane, J. E. M., Alexandre, R. S., da Silva, S. F., Pimentel, S. M., de Andrade, M. S. S., Silva, F. G. R., Branco, E. R. F., Moreira, T. R., da Silva, R. G., and de Carvalho, J. R.: Relation of El Niño and La Niña phenomena to precipitation, evapotranspiration and temperature in the Amazon basin, Science of the Total Environment, 651, 1639–1651, https://doi.org/10.1016/j.scitotenv.2018.09.242, 2019.

Muñoz-Sabater, J., Dutra, E., Agustí-Panareda, A., Albergel, C., Arduini, G., Balsamo, G., Boussetta, S., Choulga, M., Harrigan, S., Hersbach, H., Martens, B., Miralles, D. G., Piles, M., Rodríguez-Fernández, N. J., Zsoter, E., Buontempo, C., and Thépaut, J. N.: ERA5-Land: A state-of-the-art global reanalysis dataset for land applications, Earth System Science Data, 13, 4349–4383, https://doi.org/10.5194/essd-13-4349-2021, 2021.

O'Connor, J., Santos, M. J., Rebel, K. T., and Dekker, S. C.: The influence of water table depth on evapotranspiration in the Amazon arc of deforestation, Hydrology and Earth System Sciences, 23, 3917–3931, https://doi.org/10.5194/hess-23-3917-2019, 2019.

Olmo, M. E., Espinoza, J. C., Bettolli, M. L., Sierra, J. P., Junquas, C., Arias, P. A., Moron, V., and Balmaceda-Huarte, R.: Circulation Patterns and Associated Rainfall Over South Tropical South America: GCMs Evaluation During the Dry-To-Wet Transition Season, Journal of Geophysical Research: Atmospheres, 127, https://doi.org/10.1029/2022JD036468, 2022.

Pabón, J. and Dorado, J.: INTRASEASONAL VARIABILITY OF RAINFALL OVER NORTHERN SOUTH AMERICA AND CARIBBEAN REGION, Earth Sciences Research Journal, 12, 194–212, 2008.

505 Paccini, L., Hohenegger, C., and Stevens, B.: Explicit versus Parameterized Convection in Response to the Atlantic Meridional Mode, Journal of Climate, 34, 3343–3354, https://doi.org/10.1175/JCLI-D-20-0224.1, 2021.

Poveda, G., Jaramillo, A., Gil, M. M., Quiceno, N., and Mantilla, R. I.: Seasonally in ENSO-related precipitation, river discharges, soil moisture, and vegetation index in Colombia, Water Resources Research, 37, 2169–2178, https://doi.org/10.1029/2000WR900395, 2001.

Poveda, G., Waylen, P. R., and Pulwarty, R. S.: Annual and inter-annual variability of the present climate in northern South America 510 and southern Mesoamerica, Palaeogeography, Palaeoclimatology, Palaeoecology, 234, 3–27, https://doi.org/10.1016/j.palaeo.2005.10.031, 2006.

Roberts, J. M., Gash, J. H. C., Tani, M., and Bruijnzeel, L. A.: Controls on evaporation in lowland tropical rainforest, in: Forests, Water and People in the Humid Tropics, pp. 287–313, Cambridge University Press, https://doi.org/10.1017/CBO9780511535666.019, 2005.

Rodrigues, R. R. and McPhaden, M. J.: Why did the 2011-2012 La Niña cause a severe drought in the Brazilian Northeast?, Geophysical 515 Research Letters, 41, 1012–1018, https://doi.org/10.1002/2013GL058703, 2014.

Ronchail, J., Cochonneau, G., Molinier, M., Guyot, J. L., De Miranda Chaves, A. G., Guimarães, V., and De Oliveira, E.: Interannual rainfall variability in the Amazon basin and sea-surface temperatures in the equatorial Pacific and the tropical Atlantic Oceans, International Journal of Climatology, 22, 1663–1686, https://doi.org/10.1002/joc.815, 2002.

Ruiz-Barradas, A., Carton, J. A., and Nigam, S.: Structure of Interannual-to-Decadal climate variability in the tropical Atlantic sector, Journal 520 of Climate, 13, 3285–3297, https://doi.org/10.1175/1520-0442(2000)013<3285:SOITDC>2.0.CO;2, 2000.

Ruiz-Vásquez, M., Arias, P. A., and Martínez, J. A.: Enso influence on water vapor transport and thermodynamics over Northwestern South America, Theoretical and Applied Climatology, 155, 3771–3789, https://doi.org/10.1007/s00704-024-04848-3, 2024.

Seneviratne, S. I., Corti, T., Davin, E. L., Hirschi, M., Jaeger, E. B., Lehner, I., Orlowsky, B., and Teuling, A. J.: Investigating soil moisture-climate interactions in a changing climate: A review, Earth-Science Reviews, 99, 125–161, https://doi.org/10.1016/j.earscirev.2010.02.004, 525 2010.

Thoning, K. W., Tans, P. P., and Komhyr, W. D.: Atmospheric carbon dioxide at Mauna Loa Observatory: 2. Analysis of the NOAA GMCC data, 1974-1985, Journal of Geophysical Research: Atmospheres, 94, 8549–8565, https://doi.org/10.1029/JD094iD06p08549, 1989.

Torralba, V., Rodríguez-Fonseca, B., Mohino, E., and Losada, T.: The non-stationary influence of the Atlantic and Pacific niños on north Eastern South American rainfall, Frontiers in Earth Science, 3, 1–10, https://doi.org/10.3389/feart.2015.00055, 2015.

530 Towner, J., Ficchí, A., Cloke, H. L., Bazo, J., Coughlan de Perez, E., and Stephens, E. M.: Influence of ENSO and tropical Atlantic climate variability on flood characteristics in the Amazon basin, Hydrology and Earth System Sciences, 25, 3875–3895, https://doi.org/10.5194/hess-25-3875-2021, 2021.

Valencia, S., Marín, D. E., Gómez, D., Hoyos, N., Salazar, J. F., and Villegas, J. C.: Spatio-temporal assessment of Gridded precipitation products across topographic and climatic gradients in Colombia, Atmospheric Research, 285, 106 643, 535 https://doi.org/10.1016/j.atmosres.2023.106643, 2023.

Vallès-Casanova, I., Lee, S., Foltz, G. R., and Pelegrí, J. L.: On the Spatiotemporal Diversity of Atlantic Niño and Associated Rainfall Variability Over West Africa and South America, Geophysical Research Letters, 47, 1–10, https://doi.org/10.1029/2020GL087108, 2020.

Wang, K. and Dickinson, R. E.: A review of global terrestrial evapotranspiration: Observation, modeling, climatology, and climatic variability, Reviews of Geophysics, 50, 1–54, https://doi.org/10.1029/2011RG000373, 2012.

540 Williams, I. N. and Patricola, C. M.: Diversity of ENSO Events Unified by Convective Threshold Sea Surface Temperature: A Nonlinear ENSO Index, Geophysical Research Letters, 45, 9236–9244, https://doi.org/10.1029/2018GL079203, 2018.

Xie, Z., Yao, Y., Tang, Q., Liu, M., Fisher, J. B., Chen, J., Zhang, X., Jia, K., Li, Y., Shang, K., Jiang, B., Yang, J., Yu, R., Zhang, X., Guo, X., Liu, L., Ning, J., Fan, J., and Zhang, L.: Evaluation of seven satellite-based and two reanalysis global terrestrial evapotranspiration products, Journal of Hydrology, 630, 130 649, https://doi.org/10.1016/j.jhydrol.2024.130649, 2024.

545 Yoon, J. H. and Zeng, N.: An Atlantic influence on Amazon rainfall, Climate Dynamics, 34, 249–264, https://doi.org/10.1007/s00382-009-0551-6, 2010.

Zanin, P. R., Pareja-Quispe, D., and Espinoza, J.-c.: Evapotranspiration in the Amazon Basin: Couplings, hydrological memory and water feedback, Agricultural and Forest Meteorology, 352, 110 040, https://doi.org/10.1016/j.agrformet.2024.110040, 2024.

Zhang, Y., Peña-Arancibia, J. L., McVicar, T. R., Chiew, F. H., Vaze, J., Liu, C., Lu, X., Zheng, H., Wang, Y., Liu, Y. Y., Miralles,
550 D. G., and Pan, M.: Multi-decadal trends in global terrestrial evapotranspiration and its components, Scientific Reports, 6, 1–12, https://doi.org/10.1038/srep19124, 2016.

Zhao, L., Dai, A., and Dong, B.: Changes in global vegetation activity and its driving factors during 1982–2013, Agricultural and Forest Meteorology, 249, 198–209, https://doi.org/https://doi.org/10.1016/j.agrformet.2017.11.013, 2018.